Influence of Different Mechanical Parameters on the Dynamics of a Medical Device

Samir-Andrei IACOVESCU
Institute of Solid Mechanics, Romanian Academy, Bucharest, Romania, iacovescu.andrei@yahoo.ro

Polidor-Paul BRATU
Institute of Solid Mechanics, Romanian Academy, Bucharest, Romania; icecon@icecon.ro

Nicolae-Doru STĂNESCU *
National University of Science and Technology Politehnica Bucharest, Pitești University Center, Romania, nicolae.stanescu@upb.ro, s_doru@yahoo.com

* Author to whom correspondence should be addressed

Abstract: - In this paper, we will discuss the influence of some mechanical parameters on the dynamic characteristics of the motion of one medical device. The medical device is represented by a rigid solid situated on a shell (the support table). If the medical device does not move relative to the support shell, then the considered system has six degrees of freedom (4 rotations and 2 translations), otherwise, the dynamics of the mechanical system is more complicated. The mechanical system is put into the motion by a harmonic excitation given by an earthquake. We will consider in our paper only the case in which the medical device does not move with respect to the support shell. This thing can be obtained by increasing the friction force between the medical device and the shell (partial solution because it does not consider the contact loosing in the vertical direction) or by linking the medical device to the shell. Each medical device has certain specifications concerning the forces, velocities, or accelerations that it supports on different directions. Modifying the mechanical parameters of the system, the response differs from case to case, helping in the design process of the mechanical system.

Keywords: - Nonlinear stiffness, harmonic excitation, dynamic response.

1. INTRODUCTION

The moving equations of the medical device were obtained in a previous paper [1]. The main working hypotheses were:

- the medical device does not lose contact with the shell on which it is, in other words, the system does not have supplementary degrees of freedom;
- the elastic forces are non-linear ones; the case in which these forces are linear ones is only a particular case;
- the rotations of the shells are relatively small ones such that one may use the known approximations with respect to the trigonometric functions of the rotational angles.

Generally speaking, earthquakes introduce sudden motions followed by vibrations. For a medical device, one has to impose conditions relative to the amplitudes of vibrations, their velocities and accelerations, and cinematic parameters which must be situated below some values given by the manufacturer or given by the precision of the device.

The connection of the medical device to one of the shells leads to the conclusion that all cinematic conditions of the medical device transfer completely to that shell.

If the medical device is not linked to a shell, then it is possible, under certain conditions, the contact between the medical device and the support table is lost; in this way, a new mechanical system is created, the new mechanical system having a greater number of degrees of freedom. Moreover, when the contact between the medical device and the support table is restored, some shocks appear [2-34].

The problems studied in the references refer to systems with two [2] or more degrees of freedom [4, 5, 19, 20], buckling [6, 10], beams (linear or curvilinear ones) [5, 6, 9, 18, 29, 30, 32], blades [23], tyres [3], bearings [12], minimization of some components of vibrations [13, 33], reduction of weight [12], eigenvectors and eigenvalues [12], resonances [12], bifurcation [2, 14], vibration of plates [8, 28], pipes [31, 34] or bridges [4, 29], vibrations generated by earthquakes [5], effects of vibrations [7]. The problems are discussed from theoretical [2, 19, 28] and experimental points of view [3, 6, 10, 19, 27, 28], and stiffness variation [25]. Different methods are used: classical ones [2, 3, 5], matrix [11], modal analysis [15, 22], group theory [17, 26], zig-zag theory [16], topology [12, 17], finite elements [4, 18, 24], transfer matrix [21]. Authors obtain the steady state solutions [20, 22], reduction of vibrations (see [10] for natural frequencies), displacements for nonlinear vibration [8, 9], and optimization [11].

Some aspects concerning the behavior of medical devices in case of earthquakes are given in [35].

2. MECHANICAL MODEL

The system is captured in Fig. 1.

We assume that we know the functions $z_1 = z_1(t)$, $\psi_1 = \psi_1(t)$, $\theta_1 = \theta_1(t)$ (the vertical displacement and rotations of the first shell).

The equations of motion of the shells of the system are given by [1]

$$m_2 \ddot{z}_2 = f_{2131}^d - f_{1121}^d + f_{2232}^d - f_{1222}^d + f_{2333}^d - f_{1323}^d + f_{2434}^d - f_{1424}^d - m_2 g, \tag{1}$$

$$J_{x_2}^{(2)} \ddot{\psi}_2 = -\left[\left(f_{2131}^d - f_{1121}^d\right) + \left(f_{2232}^d - f_{1222}^d\right) - \left(f_{2333}^d - f_{1323}^d\right) - \left(f_{2343}^d - f_{1424}^d\right)\right] l_1, \tag{2}$$

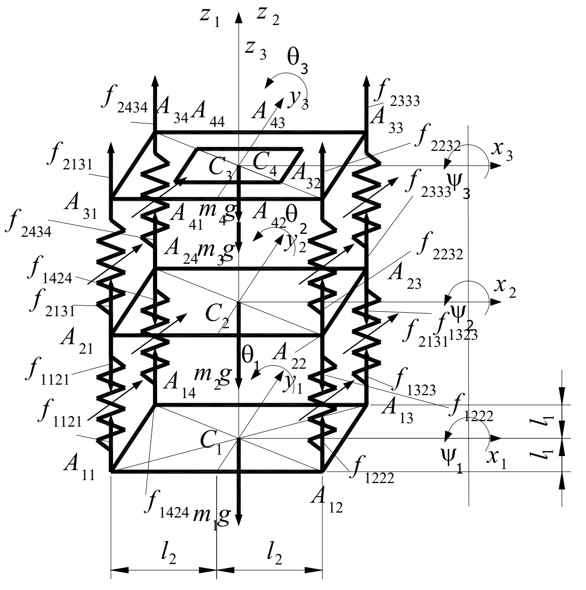

Figure 1. Mechanical system [1].

$$J_{y_2}^{(2)} \ddot{\theta}_2 = -\left[-\left(f_{2131}^d - f_{1121}^d\right) + \left(f_{2232}^d - f_{1222}^d\right) + \left(f_{2333}^d - f_{1323}^d\right) - \left(f_{2343}^d - f_{1424}^d\right)\right] l_2, \tag{3}$$

$$\left(m_3 + m_4\right) \ddot{z}_3 = -f_{2131}^d - f_{2232}^d - f_{2333}^d - f_{2434}^d - \left(m_3 + m_4\right) g, \tag{4}$$

$$J_{x_3}^{(3)} \ddot{\psi}_3 = \left(f_{2131}^d + f_{2232}^d - f_{2333}^d - f_{2343}^d\right) l_1, \tag{5}$$

$$J_{y_3}^{(3)} \ddot{\theta}_3 = \left(-f_{2131}^d + f_{2232}^d + f_{2333}^d - f_{2434}^d\right) l_2, \tag{6}$$

where

$$f_{2131}^d = k_{21}\left[\left(z_3 - z_2\right) - \left(\psi_3 - \psi_2\right) l_1 + \left(\theta_3 - \theta_2\right) l_2\right] + k_{21}^*\left[\left(z_3 - z_2\right) - \left(\psi_3 - \psi_2\right) l_1 + \left(\theta_3 - \theta_2\right) l_2\right]^3, \tag{7}$$

$$f_{2232}^d = k_{22}\left[\left(z_3 - z_2\right) - \left(\psi_3 - \psi_2\right) l_1 - \left(\theta_3 - \theta_2\right) l_2\right] + k_{22}^*\left[\left(z_3 - z_2\right) - \left(\psi_3 - \psi_2\right) l_1 - \left(\theta_3 - \theta_2\right) l_2\right]^3, \tag{8}$$

$$f_{2333}^d = k_{23}\left[\left(z_3 - z_2\right) + \left(\psi_3 - \psi_2\right) l_1 - \left(\theta_3 - \theta_2\right) l_2\right] + k_{23}^*\left[\left(z_3 - z_2\right) + \left(\psi_3 - \psi_2\right) l_1 - \left(\theta_3 - \theta_2\right) l_2\right]^3, \tag{9}$$

$$f_{2434}^d = k_{24}\left[\left(z_3 - z_2\right) + \left(\psi_3 - \psi_2\right) l_1 + \left(\theta_3 - \theta_2\right) l_2\right] + + k_{24}^*\left[\left(z_3 - z_2\right) + \left(\psi_3 - \psi_2\right) l_1 + \left(\theta_3 - \theta_2\right) l_2\right]^3, \tag{10}$$

$$f_{1121}^d = k_{11}\left[\left(z_2 - z_1\right) - \left(\psi_2 - \psi_1\right) l_1 + \left(\theta_2 - \theta_1\right) l_2\right] + k_{11}^*\left[\left(z_2 - z_1\right) - \left(\psi_2 - \psi_1\right) l_1 + \left(\theta_2 - \theta_1\right) l_2\right]^3, \tag{11}$$

$$f_{1222}^d = k_{12}\left[\left(z_2 - z_1\right) - \left(\psi_2 - \psi_1\right) l_1 - \left(\theta_2 - \theta_1\right) l_2\right] + k_{12}^*\left[\left(z_2 - z_1\right) - \left(\psi_2 - \psi_1\right) l_1 - \left(\theta_2 - \theta_1\right) l_2\right]^3, \tag{12}$$

$$f_{1323}^d = k_{13}\left[\left(z_2 - z_1\right) + \left(\psi_2 - \psi_1\right) l_1 - \left(\theta_2 - \theta_1\right) l_2\right] + k_{13}^*\left[\left(z_2 - z_1\right) + \left(\psi_2 - \psi_1\right) l_1 - \left(\theta_2 - \theta_1\right) l_2\right]^3, \tag{13}$$

$$f_{1424}^d = k_{14}\left[\left(z_2 - z_1\right) + \left(\psi_2 - \psi_1\right) l_1 + \left(\theta_2 - \theta_1\right) l_2\right] + k_{14}^*\left[\left(z_2 - z_1\right) + \left(\psi_2 - \psi_1\right) l_1 + \left(\theta_2 - \theta_1\right) l_2\right]^3. \tag{14}$$

where f_{ijkj}^d signifies the force in the non-linear spring between the points A_{ij} and A_{kj}, the superior index d marking the dynamical case, l_1 and l_2 are the dimensions of the shells, ψ_i and θ_i are the rotational angles, m_3 and m_4 are the masses of the last shell, respectively medical device, while J_{x_i} and J_{y_i} are the known moments of inertia.

The rotations are considered to be small; one may make the well-known approximations $\sin\alpha \approx \alpha$, $\cos\alpha \approx 1$.

3. NUMERICAL STUDY

For the numerical simulation, we will assume the following standard values:

- the number of iterations $n_{iter} = 12000$;
- the increment of time $dtime = 10^{-3}[\mathrm{s}]$;
- the lengths of bars $l_1 = 0.225[\mathrm{m}]$, $l_2 = 0.2\,[\mathrm{m}]$, $L_{12} = 0.45[\mathrm{m}]$, $L_{23} = 0.45[\mathrm{m}]$;
- the masses $m_1 = 5[\mathrm{kg}]$, $m_2 = 15[\mathrm{kg}]$, $m_3 = 15[\mathrm{kg}]$, $m_4 = 20[\mathrm{kg}]$;
- the elastic constants (linear components) $k_{11} = k_{12} = k_{13} = k_{14} = 12.5\times10^3[\mathrm{N/m}]$, respectively $k_{21} = k_{22} = k_{23} = k_{24} = 12.5\times10^3[\mathrm{N/m}]$;
- the non-linear components of the elastic constants $k_{11}^* = k_{12}^* = k_{13}^* = k_{14}^* = 10^6\left[\mathrm{N/m^3}\right]$, respective $k_{21}^* = k_{22}^* = k_{23}^* = k_{24}^* = 10^6\left[\mathrm{N/m^3}\right]$. They characterize the non-linear components of the elastic force, non-linear components being given by third power of deformation;
- the excitations

$$z_1(t) = \begin{cases} z_1^0 \sin(\omega_{1z_1} t), \text{for } 0 \le t \le 6[\mathrm{s}], \\ 0\,, \text{otherwise}, \end{cases} \quad (15)$$

$$\theta_1(t) = \begin{cases} \theta_1^0 \sin(\omega_{1\theta_1} t), \text{for } 0 \le t \le 6[\mathrm{s}], \\ 0\,, \text{otherwise}, \end{cases} \quad (16)$$

$$\psi_1(t) = \begin{cases} \psi_1^0 \sin(\omega_{1\psi_1} t), \text{for } 0 \le t \le 6[\mathrm{s}], \\ 0\,, \text{otherwise}, \end{cases} \quad (17)$$

where the pulsations are $\omega_{1z_1} = \pi[\mathrm{rad/s}]$, $\omega_{1\theta_1} = \pi[\mathrm{rad/s}]$, $\omega_{1\psi_1} = \pi[\mathrm{rad/s}]$;

- the amplitude of the oscillations $z_1^0 = 0.25[\mathrm{m}]$, $\psi_1^0 = 0.001[\mathrm{rad}]$, $\theta_1^0 = 0.001[\mathrm{rad}]$;
- the moments of inertia with respect to the axis x_2, $J_{x_2} = \dfrac{m_2 l_1^2}{12} = 0.06328125\left[\mathrm{kgm^2}\right]$, with respect to the axis y_2, $J_{y_2} = \dfrac{m_2 l_2^2}{12} = 0.05\left[\mathrm{kgm^2}\right]$, respectively with respect to the axes x_3, and y_3, $J_{x_3} = \dfrac{(m_3 + m_4) l_1^2}{12} = 0.14765625\left[\mathrm{kgm^2}\right]$, respectively, $J_{y_3} = \dfrac{(m_3 + m_4) l_2^2}{12} = 0.11666666\left[\mathrm{kgm^2}\right]$
- gravitational acceleration $g = 9.8065\left[\mathrm{m/s^2}\right]$;
- the damping coefficients are considered to be equal: $c_{1121} = c_{1222} = c_{1323} = c_{1424} = 50[\mathrm{Ns/m}]$, $c_{2131} = c_{2232} = c_{2333} = c_{2334} = 50[\mathrm{Ns/m}]$.

In the situations with no friction and with friction 10 cases are considered (Table 1).

Table 1. Considered cases

i)	standard case
ii)	$m_4 = 10[\mathrm{kg}]$
iii)	$m_{inew} = 2m_i$, $i = \overline{1,4}$
iv)	$k_{1inew}^* = 2k_{1i}^*$, $i = \overline{1,4}$
v)	$k_{2inew}^* = 2k_{2i}^*$, $i = \overline{1,4}$
vi)	$\omega_{1z_1new} = 2\omega_{1z_1}$, $\omega_{1\psi_1new} = 2\omega_{1\psi_1}$, $\omega_{1\theta_1new} = 2\omega_{1\theta_1}$
vii)	$L_{12new} = 2L_{12}$, $L_{23new} = 2L_{23}$
viii)	$l_{inew} = 1.5l_i$, $i = \overline{1,2}$
ix)	$z_{10new} = 2z_{10}$, $\psi_{10new} = 2\psi_{10}$, $\theta_{10new} = 2\theta_{10}$
x)	$k_{ijnew}^* = 2k_{ij}^*$, $i = \overline{1,2}$, $j = \overline{1,4}$

For the situation with friction, we add another case, the eleventh one: xi) $c_{ijnew} = 2c_{ij}$, $i = \overline{1,2}$, $j = \overline{1,4}$.

We limit our study to the dynamics of the medical device, that is, the parameters z_3, ψ_3, and θ_3, and their first and second derivatives. We also assume that the medical device is always linked to the third shell (the contact is never lost).

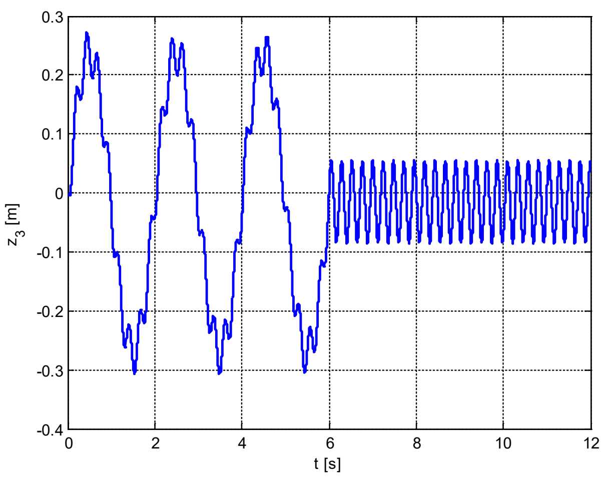

Figure 2. Time history $z_3 = z_3(t)$.

The parameters are determined in two situations: for the all interval of time ($t \in [0,\ 12][\mathrm{s}]$) or only for the last second ($t \in [11,\ 12][\mathrm{s}]$).

In Figs. 2, 3, and 4, we present the time variations of some parameters in the standard case without friction.

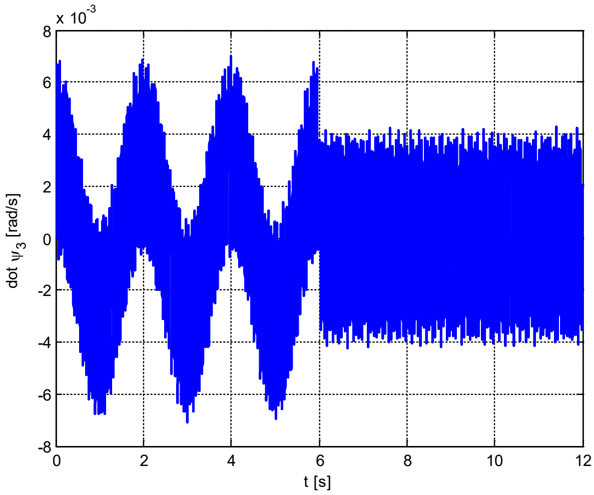

Figure 3. Time history $\dot{\psi}_3 = \dot{\psi}_3(t)$.

In order to obtain these representations, some calculation programs are realized, the output files containing different cinematic parameters (linear or angular displacements, velocities, or accelerations). The input data are those presented previously. The integration was realized using the fourth-order Runge-Kutta method, the step of iterations being $dtime = 10^{-3}[\mathrm{s}]$.

For the parameters (vertical displacement, angles of rotation) and their first derivatives (linear velocity and angular velocities), one may easily observe the existence of excitation (the first part of the interval of time). The statement is not true for the accelerations (linear and angular).

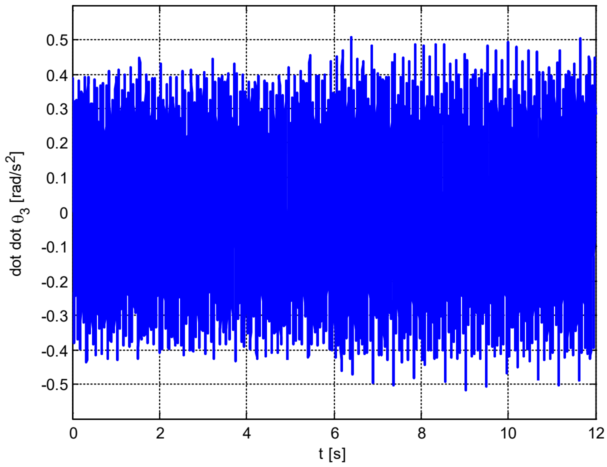

Figure 4. Time history $\ddot{\theta}_3 = \ddot{\theta}_3(t)$.

Table 2. Results of simulations (no friction)

i)	$z_{3\min} = -0.30704[\mathrm{m}],\ z_{3\max} = 0.27307[\mathrm{m}],\ \psi_{3\min} = -0.00104[\mathrm{rad}],\ \psi_{3\max} = 0.00104[\mathrm{rad}],\ \theta_{3\min} = -0.00104[\mathrm{rad}],\ \theta_{3\max} = 0.00104[\mathrm{rad}]$
ii)	$z_{3\min} = -0.29721[\mathrm{m}],\ z_{3\max} = 0.27362[\mathrm{m}],\ \psi_{3\min} = -0.00103[\mathrm{rad}],\ \psi_{3\max} = 0.00103[\mathrm{rad}],\ \theta_{3\min} = -0.00103[\mathrm{rad}],\ \theta_{3\max} = 0.00103[\mathrm{rad}]$
iii)	$z_{3\min} = -0.34268[\mathrm{m}],\ z_{3} = 0.27032[\mathrm{m}],\ \psi_{3\min} = -0.00106[\mathrm{rad}],\ \psi_{3\max} = 0.00106[\mathrm{rad}],\ \theta_{3\min} = -0.00106[\mathrm{rad}],\ \theta_{3\max} = 0.00106[\mathrm{rad}]$
iv)	$z_{3\min} = -0.30719[\mathrm{m}],\ z_{3\max} = 0.27370[\mathrm{m}],\ \psi_{3\min} = -0.00104[\mathrm{rad}],\ \psi_{3\max} = 0.00104[\mathrm{rad}],\ \theta_{3\min} = -0.00104[\mathrm{rad}],\ \theta_{3\max} = 0.00104[\mathrm{rad}]$
v)	$z_{3\min} = -0.30703[\mathrm{m}],\ z_{3\max} = 0.27261[\mathrm{m}],\ \psi_{3\min} = -0.00104[\mathrm{rad}],\ \psi_{3\max} = 0.00104[\mathrm{rad}],\ \theta_{3\min} = -0.00104[\mathrm{rad}],\ \theta_{3\max} = 0.00104[\mathrm{rad}]$
vi)	$z_{3\min} = -0.34974[\mathrm{m}],\ z_{3\max} = 0.32380[\mathrm{m}],\ \psi_{3\min} = -0.00108[\mathrm{rad}],\ \psi_{3\max} = 0.00108[\mathrm{rad}],\ \theta_{3\min} = -0.00108[\mathrm{rad}],\ \theta_{3\max} = 0.00108[\mathrm{rad}]$
vii)	$z_{3\min} = -0.30704[\mathrm{m}],\ z_{3\max} = 0.27307[\mathrm{m}],\ \psi_{3\min} = -0.00104[\mathrm{rad}],\ \psi_{3\max} = 0.00104[\mathrm{rad}],\ \theta_{3\min} = -0.00104[\mathrm{rad}],\ \theta_{3\max} = 0.00104[\mathrm{rad}]$
viii)	$z_{3\min} = -0.30704[\mathrm{m}],\ z_{3\max} = 0.27307[\mathrm{m}],\ \psi_{3\min} = -0.00104[\mathrm{rad}],\ \psi_{3\max} = 0.00104[\mathrm{rad}],\ \theta_{3\min} = -0.00104[\mathrm{rad}],\ \theta_{3\max} = 0.00104[\mathrm{rad}]$
ix)	$z_{3\min} = -0.59116[\mathrm{m}],\ z_{3\max} = 0.55707[\mathrm{m}],\ \psi_{3\min} = -0.00208[\mathrm{rad}],\ \psi_{3\max} = 0.00208[\mathrm{rad}],\ \theta_{3\min} = -0.00208[\mathrm{rad}],\ \theta_{3\max} = 0.00208[\mathrm{rad}]$
x)	$z_{3\min} = -0.30696[\mathrm{m}],\ z_{3\max} = 0.27630[\mathrm{m}],\ \psi_{3\min} = -0.00104[\mathrm{rad}],\ \psi_{3\max} = 0.00104[\mathrm{rad}],\ \theta_{3\min} = -0.00104[\mathrm{rad}],\ \theta_{3\max} = 0.00104[\mathrm{rad}]$

Table 3. Results of simulations (with friction, last second)

i)	$z_{3\min} = -0.01662[\mathrm{m}]$, $z_{3\max} = -0.01651[\mathrm{m}]$, $\psi_{3\min} = 0[\mathrm{rad}]$, $\psi_{3\max} = 0[\mathrm{rad}]$, $\theta_{3\min} = 0[\mathrm{rad}]$, $\theta_{3\max} = 0[\mathrm{rad}]$
ii)	$z_{3\min} = -0.01271[\mathrm{rad}]$, $z_{3\max} = -0.01270[\mathrm{rad}]$, $\psi_{3\min} = 0[\mathrm{rad}]$, $\psi_{3\max} = 0[\mathrm{rad}]$, $\theta_{3\min} = 0[\mathrm{rad}]$, $\theta_{3\max} = 0[\mathrm{rad}]$
iii)	$z_{3\min} = -0.03458[\mathrm{m}]$, $z_{3\max} = -0.03080[\mathrm{m}]$, $\psi_{3\min} = 0[\mathrm{rad}]$, $\psi_{3\max} = 0[\mathrm{rad}]$, $\theta_{3\min} = 0[\mathrm{rad}]$, $\theta_{3\max} = 0[\mathrm{rad}]$
iv)	$z_{3\min} = -0.01655[\mathrm{m}]$, $z_{3\max} = -0.01646[\mathrm{m}]$, $\psi_{3\min} = 0[\mathrm{rad}]$, $\psi_{3\max} = 0[\mathrm{rad}]$, $\theta_{3\min} = 0[\mathrm{rad}]$, $\theta_{3\max} = 0[\mathrm{rad}]$
v)	$z_{3\min} = -0.01660[\mathrm{m}]$, $z_{3\max} = -0.01649[\mathrm{m}]$, $\psi_{3\min} = 0[\mathrm{rad}]$, $\psi_{3\max} = 0[\mathrm{rad}]$, $\theta_{3\min} = 0[\mathrm{rad}]$, $\theta_{3\max} = 0[\mathrm{rad}]$
vi)	$z_{3\min} = -0.01668[\mathrm{m}]$, $z_{3\max} = -0.01646[\mathrm{m}]$, $\psi_{3\min} = 0[\mathrm{rad}]$, $\psi_{3\max} = 0[\mathrm{rad}]$, $\theta_{3\min} = 0[\mathrm{rad}]$, $\theta_{3\max} = 0[\mathrm{rad}]$
vii)	$z_{3\min} = -0.01662[\mathrm{m}]$, $z_{3\max} = -0.01651[\mathrm{m}]$, $\psi_{3\min} = 0[\mathrm{rad}]$, $\psi_{3\max} = 0[\mathrm{rad}]$, $\theta_{3\min} = 0[\mathrm{rad}]$, $\theta_{3\max} = 0[\mathrm{rad}]$
viii)	$z_{3\min} = -0.01662[\mathrm{m}]$, $z_{3\max} = -0.01651[\mathrm{m}]$, $\psi_{3\min} = 0[\mathrm{rad}]$, $\psi_{3\max} = 0[\mathrm{rad}]$, $\theta_{3\min} = 0[\mathrm{rad}]$, $\theta_{3\max} = 0[\mathrm{rad}]$
ix)	$z_{3\min} = -0.01667[\mathrm{m}]$, $z_{3\max} = -0.01647[\mathrm{m}]$, $\psi_{3\min} = 0[\mathrm{rad}]$, $\psi_{3\max} = 0[\mathrm{rad}]$, $\theta_{3\min} = 0[\mathrm{rad}]$, $\theta_{3\max} = 0[\mathrm{rad}]$
x)	$z_{3\min} = -0.01653[\mathrm{m}]$, $z_{3\max} = -0.01643[\mathrm{m}]$, $\psi_{3\min} = 0[\mathrm{rad}]$, $\psi_{3\max} = 0[\mathrm{rad}]$, $\theta_{3\min} = 0[\mathrm{rad}]$, $\theta_{3\max} = 0[\mathrm{rad}]$
xi)	$z_{3\min} = -0.01657[\mathrm{m}]$, $z_{3\max} = -0.01657[\mathrm{m}]$, $\psi_{3\min} = 0[\mathrm{rad}]$, $\psi_{3\max} = 0[\mathrm{rad}]$, $\theta_{3\min} = 0[\mathrm{rad}]$, $\theta_{3\max} = 0[\mathrm{rad}]$

Analyzing the results of the simulation, we may state in each case the results presented in Table 2 for the cases without friction.

For the case with friction, we present only the results for the last second of simulations. The results are captured in Table 3.

In these tables, we limited ourselves only to the maximum and minimum values of the linear and angular displacements.

4. CONCLUSIONS

One may easily observe that there exist no symmetric vibrations even in the case without friction. The situations in which the maximum and minimum values of the amplitudes are equal are particular cases. This conclusion is more obvious for velocities and accelerations (values which are not given in this paper).

There are some variations in parameters that do not lead to the variations of some amplitudes' parameters (see, for instance, case iv), for which $\psi_{3\min}$, $\psi_{3\max}$, , $\theta_{3\min}$, $\theta_{3\max}$ have the same values as in the standard case (case i).

On the other hand, some variations in parameters may lead to the increase of the amplitudes of vibrations (see, for instance, case vi) and case i)), while the variations of other parameters lead to the decrease of the amplitudes of vibrations (see, for instance, case ii) and case i)).

Some variations of the parameters lead to the same variations of amplitudes for certain vibrations (see, for instance, case iv) case v) and case vii), where we obtained the same results for $\psi_{3\min}$, $\psi_{3\max}$, $\theta_{3\min}$ and $\theta_{3\max}$.

As it results from case ix) the changing of the initial conditions may lead to dramatic changes in the amplitudes of vibrations. We may state that the system is very sensitive to initial conditions.

The situations are similar when we consider only the last second of the simulation.

In the cases with friction, the values of the amplitudes are smaller. The values equal to 0 appear due to the representation of numbers in a computer; they are very small numbers that may be considered equal to zero. In addition, the same sign for the minimum value and maximum value of certain vibrations proofs that the oscillations do not pass to 0 positions any more.

The last case, when the minimum and the maximum values of the parameter z_3 are equal, shows that the increase of the damping coefficient may lead to the cancellation (in the precision of the computer) of vibrations.

The dynamics of the medical device was studied, and the influence of different mechanical parameters was described. More studies must be realized concerning the force between the third shell and the medical device (the contact may be lost at all points A_{41}, A_{42}, A_{43}, and A_{44}, or may be lost only two or three point).

In our next papers, we will discuss the influence of the mechanical parameters (those considered here, at which we may add some other new ones) on linear and angular velocities and accelerations.

REFERENCES

[1] Iacovescu, S.-A., Bratu, P.-P., Stănescu, N.-D., Dynamics of a system with non-linear cubic stiffness, *Applied Sciences* (sent for publication).

[2] Bajaj, A. K., Davies, P., Benerjee, B., Non-Stationary Responses in Externally Excited Two-Degrees-of-Freedom Nonlinear Systems with 1:2 Internal Resonance, *Journal of Vibration and Control*, 2004, Vol. 10, pp. 1663-1697.

[3] Tsinias, V., Mavros, G., Efficient experimental identification of three-dimensional tyre structural properties, *Proceedings of the Institution of Mechanical Engineers, Part D: Journal of Automobile Engineering*, 2019, Vol. 233(1), pp. 88-106.

[4] Ju, S.-H., Derailment of trains moving on lead rubber bearing bridges under seismic loads, *Journal of Vibration and Control*, 2020, Vol. 26(19-20), pp. 1646-1665.

[5] Ding, J., Huang, H., Zhuang, W., Wang, C., Analysis of the response of a reinforced concrete wall structure during earthquakes using the transfer matrix method pf multibody systems, *Advances in Mechanical Engineering*, 2016, Vol. 8(5), pp. 1-25.

[6] Viet, N. V., Zaki, W., Free vibration and buckling characteristics of functionally graded beams with triple periodic minimal surface structure, *Composite Structures*, 2023, Vol. 274, paper 114342.

[7] Carillo-Munoz, M., Sharma, S., Identifying elastic wave polarization and bandgaps in periodic solid media, *International Journal of Mechanical Sciences*, 2023, Vol. 252, paper 108363.

[8] Torabi, J., Niiranen, J., Nonlinear finite element free and forced vibrations of cellular plates having lattice-type metamaterial cores: a strain gradient plate model approach, *Mechanical Systems and Signal Processing*, 2023, Vol. 192, paper 110224.

[9] Yang, J., Jacobs, G., Kramer, A., Drichel, P., Liu, C., Investigation of the tire in-plane vibration property using an improved ring model, *Journal of Sound and Vibration*, 2020, Vol. 478, paper 115350.

[10] Jeon, M.-H., Cho, H.-J., Sim, C.-H., Kim, Y.-J., Lee, M.-Y., Kim, I.-G., Park, J. S., Experimental and numerical approach for predicting global buckling load of pressurized unstiffened cylindrical shells using vibration correlation technique, *Composite Structures*, 2023, Vol. 305, paper 116460.

[11] Niu, B., Feng, N., Lund, E., Leng, Y., Discrete material optimization of composite structures subjected to initial excitation for minimum residual vibration, *Thin-Walled Structures*, 2022, Vol. 173, paper 108901.

[12] Mélot, A., Benaïcha, Y., Rigaud, E., Perret-Liaudet, J., Thouverez, F., Effect of gear topology discontinuities on the nonlinear dynamic response of a multi-degree-of-freedom gear train, *Journal of Sound and Vibration*, 2022, Vol. 516, paper 116495.

[13] Gomez, E. R., Kari, L., Lopez Arteaga, I., Powertrain shuffle-mode resonance suppression by means of flywheel mounted torsichrone centrifugal pendulum vibration absorbers, *Journal of Sound and Vibration*, 2022, Vol. 534, paper 117014.

[14] Zhang, W., Gu, X. J., Zhang, Y. F., New modeling on vibrations and bifurcations of FGGP reinforced pretwisted composite rotating blade under axial aerodynamic force: Theoretical and numerical researches, *Thin-Walled Structures*, ***2023***, Vol. 184, paper 110523.

[15] Bui, T. A., Lardeur, P., Oudjene, M., Park, J., Numerical modelling of the variability of the vibration frequencies of multi-layered timber structures using the modal stability procedure, *Composite Structures*, 2022, Vol. 285, paper 115226.

[16] Lewandowski, R., Litewka, P., Nonlinear harmonic vibrations of laminate plates with viscoelastic layers using refined zig-zag theory. Part 1 – Theoretical background, *Composite Structures*, 2023, Vol. 320, paper 117200.

[17] Xue, L., Wen, G., Wang, H., Liu, J., Eigenvectors-guided topology optimization to control the mode shape and suppress the vibration of the multi-material plate, *Computer Methods in Applied Mechanics and Engineering*, 2022, Vol. 391, paper 114560.

[18] Wei, G., Lardeur, P., Druesne, F., Free vibration analysis of thin to thick straight or curved beams by a solid-3D beam finite element method, *Thin-Walled Structures*, 2023, Vol. 191, paper 111028.

[19] Gad-el-Hak, I., Mureithi, N., Karazis, K., Williams, G., Principal component analysis of vibration response of a rod bundle subjected to jet cross-flow, *Journal of Sound and Vibration*, 2023, Vol. 550, paper 117592.

[20] Masri, S. F., Caffrey, J. P., Response of a multi-degree-of-freedom system with a pounding vibration neutralizer to harmonic and random excitation, *Journal of Sound and Vibration*, 2020, Vol. 481, paper 115427.

[21] Lu, H., Rui, X., Zhang, X., Transfer matrix method for linear vibration analysis of flexible multibody systems, *Journal of Sound and Vibration*, 2023, Vol. 549, paper 117565.

[22] Pei, X., Ravi, S. K., Dong, P., Li, X., Zhou, X., A multi-axial vibration fatigue evaluation procedure for welded structures in frequency domain, *Mechanical Systems and Signal Processing*, 2022, Vol. 167, paper 108516.

[23] Aghayari, J., Bab, S., Safarpour, P., Rahi, A., A novel modal vibration reduction of a disk-blades of a turbine using nonlinear energy sinks on the disk, *Mechanism and Machine Theory*, 2020, Vol. 155, paper 104048.

[24] Treyssède, F., Cesbron, J., Waveguide finite element modelling for broadband vibration analysis of rotating and prestressed circular structures: Application to tyres, *Journal of Sound and Vibration*, 2023, Vol. 543, paper 117361.

[25] Ben Lassoued, M. A., Ross, A., Michon, G., Vibration confinement and localization patterns in weakly coupled oscillators with parameter gradients, *Journal of Sound and Vibration*, 2023, Vol. 549, paper 117590.

[26] Dong, B., Parker, R. G., Vibration of general symmetric systems using group theory, *Journal of Sound and Vibration*, 2021, Vol. 503, paper 116087.

[27] Li, M., Chen, X., Luo, S., Ma, W., Dinggang, G., Analysis on abnormal low-frequency vertical vibration of medium–low-speed maglev vehicle, *Mechanical Systems and Signal Processing*, 2023, Vol. 200, paper 110510.

[28] Li, H., Liu, Y., Shi, X., Wang, Z., Wang, X., Xiong, J., Guan, Z., Nonlinear vibrations of all-composite sandwich plates with a hexagon honeycomb core: Theoretical and experimental investigations, *Composite Structures*, 2023, Vol. 305, paper 116512.

[29] Zangeneh, A., Museros, P., Pacoste, C., Karoumi, R., Free vibration of viscoelastically supported beam bridges under moving loads: Closed-form formula for maximum resonant response, *Engineering Structures*, 2021, Vol. 244, paper 112759.

[30] Nikolić, A., Šalinić, S., Free vibration analysis of 3D non-uniform beam: the rigid segment approach. *Engineering Structures*, 2020, Vol. 222, paper 110796.

[31] Guo, X., Gao, P., Ma, H., Li, H., Wang, B., Han, Q., Wen, B., Vibration characteristics analysis of fluid-conveying pipes concurrently subjected to base excitation and pulsation excitation, *Mechanical Systems and Signal Processing*, 2023, Vol. 189, paper 110086.

[32] Adam, C., Ladurner, D., Furtmüller, T., Free and forced small flexural vibrations of slightly curved slender composite beams with interlayer slip, *Thin-Walled Structures*, 2022, Vol. 180, paper 109857.

[33] Laghfiri, H., Lamdouar, N., Abbas, S., Boudi, E. M., Periodic wave impeding barrier as a countermeasure of ground vibration, *Advances in Mechanical Engineering*, 2023, Vol. 15, Issue 8, pp. 1–11.

[34] Blasi, G., Perrone, D., Aiello, M. A., Parametric investigation on the response of suspended piping systems to tri-directional seismic excitation, *Engineering Structures*, 2023, Vol. 293, paper 116713

[35] Mazza, F., In-plane and out-of-plane nonlinear seismic response of masonry infills for hospitals retrofitted with hysteretic damped braces, *Soil Dynamics and Earthquake Engineering*, 2021, Vol. 148, paper 106803.